I J R B A T, Issue (XI) Vol (II) May 2023 : 99-114 e-ISSN 2347 – 517X
A Double-Blind Peer Reviewed & Refereed Journal OPEN ACCESS Original Article

INTERNATIONAL JOURNAL OF RESEARCHES IN BIOSCIENCES, AGRICULTURE AND TECHNOLOGY
 www.ijrbat.in

TIME-FRACTIONAL CATTANEO-TYPE THERMOELASTIC INTERIOR-BOUNDARY VALUE PROBLEM WITHIN A RIGID BALL

Geeta Dhameja[1] and Lalsingh Khalsa[2]

1Department of Mathematics, M.G. College, Armori, Gadchiroli, India
Corresponding Email: dhameja.geeta0311@gmail.com, lalsinghkhalsa@yahoo.com

Communicated : 12.01.2023 | Revision : 16.02.2023 & 23.02.2023 Accepted : 22.03.2023 | Published : 30.05.2023

ABSTRACT:
The paper discusses the solution of an interior-boundary value problem of one-dimensional time-fractional Cattaneo-type heat conduction and its stress fields for a rigid ball. The interior value problem describes the dependence of the boundary conditions within the ball's inner plane at any instant with a prescribed temperature state, in contrast to the exterior value problem, which relates the known surface temperature as boundary conditions. A single-phase-lag equation with Caputo fractional derivatives is proposed to model the heat equation in a medium subjected to time-dependent physical boundary conditions. The application of the finite spherical Hankel and Laplace transform technique to heat conduction is discussed. The influence of the fractional-order parameter and the relaxation time is examined on the temperature fields and their related stresses. The findings show that the slower the thermal wave, the bigger the fractional-order setting, and the higher the period of relaxation, the slower the heat flux propagates.

Keywords :- Fractional Cattaneo-type equation, fractional calculus, non-Fourier heat conduction, ball, thermal stress, integral transform.

INTRODUCTION :

Many papers deal with the temperature and thermal stress fields due to body heating in the theory of thermal stress. The determination of either heat flux or temperature at interior points is deduced from the known temperature at the surface. In contrast, there is a subset of cases in which the temperature distribution at some interior points is known. It is required to determine either temperature or heat flux on the surface, commonly named interior value problems (or so-called inverse temperature field problems). In order to find the unknown functions that characterize the boundary conditions, one assumes that (i) a kind of the boundary conditions are known, (ii) initial conditions are known, (iii) other boundary conditions - if any exist - are known, (iv) specific mechanical or thermal internal responses inside the object are known. When it comes to determining the transient temperature or heat flux distribution at a surface where temperature or heat flux measurements are impossible or problematic, then inverse temperature field problems will have a practical and useful application. Such situations have been documented several times in literature; therefore, few of them are quoted here.

Stolz [1] suggested the first solutions for the inverse heat problems with integral equations and numerical methods. Necsulescu [2], Woodbury [3], Özışık [4] and Beck [5] have developed several methods of interior-boundary value heat conduction problems for various forms of boundary conditions. Torsten et al. [6] solved the linear inverse heat conduction problem to reconstruct unknown heat flux at the boundary for two- and three-dimensional problems. Lu and Tervola [7] developed an empirical approach to heat conduction in a composite slab when subjected to periodic temperature changes. Khobragade et al. [8] investigated an inverse transient thermoelastic problem in which we need to determine the

http://doi.org/10.29369/ijrbat.2023.02.1.0015

unknown temperature, displacement and stress function on the outer curved surface of a thin annular disc when the interior heat flux is known using integral transform techniques. Woodfield et al. [8] solved the inverse heat conduction problems analytically using the Laplace transform when it has a given far-field boundary state. Pourgholi and Rostamian [9] used the Tikhonov regularization approach to provide a numerical solution to the one-dimensional inverse heat conduction problems. Danaila and Chira [10] proposed the solution to the inverse one-dimensional heat conduction problem; they intend to estimate the unsteady boundary state on the right side using two techniques: first, to combine the gradient approach with an adjunct issue for the estimate of gradient function, and second, to regularize Tikhonov for hyperbolization of the equation of heat conduction. Ivanchov and Kinash [11] found the inverse problem in a rectangle, the heat conduction equation with an unknown coefficient, as a function of time and space variables using the Green function. Chen et al. [12] used the one-dimensional problem of inverse heat conduction to measure the surface temperature; they used a nonlinear form of calculation with an integral equation. Chang et al. [13] split them into two main solving groups in their study paper on the computing approaches used for inverse heat conduction problems: mesh techniques and meshless algorithms.

Recently, the fractional-order concept has been put in use to obtain better performance of the system. The Laplace transform was used by Kukla and Siedlecka [14] to solve fractional heat conduction in a two-layer slab. Meanwhile, technological development and innovation in research helped bring about a revolution by applying heat relaxation time to the non-equilibrium heat conduction system [15-18]. Cattaneo [19] and Vernotte [20] have summed the heat relaxation time to a partial heat flux time derivative. In the meantime, Compte and Metzler [21] focused on four different generalizations of the Cattaneo telegraph equations, each of which was accompanied by a different scheme: continuous-time random walks, nonlocal transport theory, and delayed flux-force relation. According to Povstenko [22], the time-fractional Cattaneo heat conduction equation derived from the Fourier law's time-non-local generalization using multiple kernels is a function Mittag-Leffler form's related thermal stress theory. Mishra and Rai [23] obtained the fractional single-phase heat conductivity function by applying the Taylor series's fractional formula to the single-phase heat conductivity function. The mathematical solutions of the fractional Cattaneo-Vernotte heat conduction problem with Neumann boundary conditions have recently been obtained in a semi-infinite medium by a few researchers [24-29]. Nevertheless, the interior-boundary value problem of time-fractional Cattaneo-type heat conduction with the physical Robin-type boundary state was less studied, based on the fractional model Cattaneo-Vernotte. Hence, this paper investigates the analytical solution for Cattaneo's time-fractional heat conduction in a finite one-dimensional ball under Robin-type conditions and analyzes the heat conduction mechanism, which differs from the fractional-order parameters.

The outline of the paper consists of five parts. In part 2, the basic set of equations for the mathematical modelling of the single-phase-lag heat conduction equation of the fractional Cattaneo-type model are stated. Then, a way of obtaining the exact solutions of time-fractional Cattaneo heat conduction analysis for such a problem is briefly presented. The final parts contain an analysis of the outcomes and discussion concerning the particular case.

http://doi.org/10.29369/ijrbat.2023.02.1.0015

Conclusive findings are summed up in the last part

Mathematical model

Formulation of fractional Cattaneo-type heat conduction equation

The classical Fourier's law of heat conduction [30]

$$q(t) = -k\nabla T(t) \quad (1)$$

in which $q(t)$ is the heat flux vector represents heat flow per unit time per unit area of the isothermal surface, t is the time, and k is the thermal conductivity of the material, ∇ is the spatial gradient operator, and T is the temperature gradient is a vector normal to the surface, respectively. Since the heat flux points to decreasing temperature, the minus sign is involved in making the heat flow a positive quantity. When the heat flux is in W/m^3, and the temperature gradient is in ^{o}C/m, the thermal conductivity has W/(m^{o}C).

Introduction of single-phase-lag to evade discrepancy between the mathematical model [19,20] and the experimental observations [31], and this extension turns the parabolic into a hyperbolic equation

$$q(t) + \zeta\frac{\partial q(t)}{\partial t} = -k\nabla T(t) \quad (2)$$

Here the flux relaxes with some given characteristic time constant ζ is the phase lag of the heat flux or so-called relaxation time. Consequently, the propagation velocity is finite. As a limiting case $\zeta \to 0$, one recovers Fourier's law with an infinitely fast propagation. The Laplace transform allows us to rewrite Eq. (2) as a time-non-local constitutive equation with the exponential kernel [22] as

$$q(t) = -\frac{k}{\zeta}\int_0^t \exp\left(-\frac{t-\tau}{\zeta}\right)\nabla T(\tau)\,d\tau \quad (3)$$

By combining Eq. (1) with the conservation law of energy [32], leads to

$$-\nabla\cdot q(t) + Q = \rho C_v\frac{\partial T(t)}{\partial t} \quad (4)$$

leads to the single-phase-lag heat conduction equation as

$$\frac{\partial^2 T(t)}{\partial t^2} + \frac{1}{\zeta}\frac{\partial T(t)}{\partial t} = \frac{\kappa}{\zeta}\left(\Delta T(t) + \frac{Q}{k}\right) \quad (5)$$

where thermal diffusivity is $\kappa = k/\rho C_v$, k being the conductivity of the material, ρ is the density of the material, C_v is the specific heat capacity, Q represents the uniform heat generation inside the material, and the square root of the ratio κ/ζ defines the finite speed within the medium, respectively.

Recently, a kind of generalization of Eq. (2) and (4) consisting of replacing the classical integer-order derivative with fractional order can be referred to in literature [21,22] and the reference therein. Next, we consider the generalization of Eq. (6) in the form

$$\frac{\partial q(t)}{\partial t} + \zeta\frac{\partial^{\alpha-1} q(t)}{\partial t^{\alpha-1}} = -k\nabla T(t),\ 0 < \alpha \le 1 \quad (6)$$

in which the fractional Caputo derivative of order α with a lower limit zero

$$\frac{\partial^\alpha f(t)}{\partial t^\alpha} = {}_0^C D_t^\alpha f(t) = \begin{cases} \frac{1}{\Gamma(m-\alpha)}\int_0^t (t-\gamma)^{m-\alpha-1}\frac{\partial^m f(\gamma)}{\partial \gamma^m}d\gamma,\ m-1<\alpha<m \\ \frac{\partial^m f(t)}{\partial t^m},\ \alpha = m,\ m\in N \end{cases} \quad (7)$$

whereas the Riemann-Liouville fractional derivative is taken as

$$D_{RL}^\alpha f(t) = \frac{\partial^m}{\partial t^m}\left[\frac{1}{\Gamma(m-\alpha)}\int_0^t (t-\gamma)^{m-\alpha-1} f(\gamma)\,d\gamma\right],\ m-1<\alpha<m \quad (8)$$

The law of heat conduction proposed by Gurtin and Pipkin [33], which leads to general time-nonlocal dependence, was later modified by Povstenko [22] as

$$q(t) = -k\int_0^t K(t-\tau)\nabla T(\tau)\,d\tau \quad (9)$$

http://doi.org/10.29369/ijrbat.2023.02.1.0015

where a general heat flux history model depends on the relaxation kernel $K(t)$.

By simple calculations, Compte and Metzler [4] have shown that the generalized Cattaneo law, obtained from the following relationship

$$\frac{\partial q(t)}{\partial t}+\zeta\frac{\partial^{\alpha-1}q(t)}{\partial t^{\alpha-1}}=-k\left(\frac{\partial}{\partial t}+\zeta\frac{\partial^{\alpha-1}}{\partial t^{\alpha-1}}\right)\int_0^t K(t-\tau)\nabla T(\tau)\,d\tau \tag{10}$$

By using Leibniz's formula for the differentiation of an integral, one obtains

$$\frac{\partial q(t)}{\partial t}+\zeta\frac{\partial^{\alpha-1}q(t)}{\partial t^{\alpha-1}}=-K(0)\nabla T(t)-\int_0^t\left[\frac{\partial}{\partial t}K(t-\tau)+\zeta\frac{\partial^{\alpha-1}}{\partial t^{\alpha-1}}K(t-\tau)\right]\nabla T(\tau)\,d\tau \tag{11}$$

Now compared with Eq. (6), it appears clear that we must have $K(0)=k$ and

$$\frac{\partial}{\partial t}K(t)+\zeta\frac{\partial^{\alpha-1}}{\partial t^{\alpha-1}}K(t)=0 \tag{12}$$

By solving Eq. (12), one can obtain the relaxation function in the Laplace domain as

$$K^*(s)=\frac{k}{\zeta}\left(\frac{s^{-1}}{s^{\alpha-2}+1/\zeta}\right) \tag{13}$$

The expression in (14) can be inverted in terms of a generalized Mittag-Leffler function (see [34]) to yield

$$K(t)=\frac{k}{\zeta}t^{\alpha-4}E_{\alpha-2,\alpha-1}\left(-\frac{1}{\zeta}t^{\alpha-2}\right) \tag{14}$$

Multiplying with vector ∇ to Eq. (6), and then using Eq. (4), results in the generalized Cattaneo equation II [22]

$$\frac{\partial^2 T(r,t)}{\partial t^2}+\frac{1}{\tau}\frac{\partial^\alpha T(r,t)}{\partial t^\alpha}=\frac{\kappa}{\tau}\left(\Delta T(r,t)+\frac{Q}{k}\right) \tag{15}$$

It was also observed that only a few had paid attention to the fourth equation. Here, the authors believe that this gap could lead to generalization, taking into account the generation of internal heat sources within the body.

Analytical solution time-fractional Cattaneo heat conduction

Figure 1 shows a schematic sketch for a ball in the spherical coordinate axes *r*, *θ*, *z* is used to describe a time-fractional thermoelastic analysis. The temperature profile is assumed to be a radial coordinate's transient function independent of the tangential and azimuthal coordinates.

We assume that the temperature at every instant is given by

$$T(r,t)=\int_0^t f(t-\gamma)\theta(r,\gamma)\,d\gamma \tag{16}$$

where $\theta(r,t)$ is the basic solution to the following problem:

$$\frac{\partial^2\theta}{\partial t^2}+\frac{1}{\tau}\frac{\partial^\alpha\theta}{\partial t^\alpha}=\frac{\kappa}{\tau}\left[\frac{1}{r^2}\frac{\partial}{\partial r}\left(r^2\frac{\partial\theta}{\partial r}\right)\right]+\frac{\kappa}{\tau}\frac{Q}{k},\quad 0\le r\le a,\ 0<t<\infty,\ 0<\alpha\le 1 \tag{17}$$

subjected to zero initial and ambient conditions

$$\theta(r,t=0)=0,\ \frac{\partial}{\partial t}\theta(r,t=0)=0,\quad 0\le r\le a, 0<\alpha\le 1 \tag{18}$$

under the physical Robin boundary condition [36-38], which is a linear combination of temperature and its normal derivative along the radial direction

$$\theta(r=\xi,t)+\zeta D_{RL}^{1-\alpha}\frac{\partial\theta}{\partial r}(r=\xi,t)=q_s(t),\quad 0<\xi<a,\ 0<\alpha\le 1 \tag{19}$$

and the assumed bounded condition at the origin as

$$\lim_{r\to 0}\theta(r,t)\neq\theta_\infty \tag{20}$$

with the fact that the temperature at the ball surface, say $\theta(r=a,t)=\Theta(t)$, is unknown. Here the notation θ_∞ represents the far-field temperature, $D_{RL}^{1-\alpha}$ is the Riemann Liouville fractional derivative of the fractional-order $1-\alpha$

http://doi.org/10.29369/ijrbat.2023.02.1.0015

, $q_s(t)=q(r=0,t)=(\partial_t+\zeta D_{RL}^{1-\alpha})\,f(t)$, $f(t)=q_0\delta(t)$ is sectional prescribed heat supply, $\delta(\ )$ is the Dirac delta function and q_0 is a constant associated with delta term, respectively.

We present the function $\theta(r,t)$ in the first phase of solving this problem in the superposition of steady-state and transient solution

$$\theta(r,t)=\theta_s(r)+\theta_t(r,t) \tag{21}$$

The function $\theta_s(r)$ satisfies the steady-state differential equation

$$\frac{1}{r^2}\frac{\partial}{\partial r}\left(r^2\frac{\partial\theta_s}{\partial r}\right)+\frac{\kappa}{\tau}\frac{Q}{k}=0 \tag{22}$$

subjected to non-homogeneous boundary conditions as given in Eq. (19).

Solving Eq. (22) leads

$$\theta_s(r)=-\frac{\kappa}{\tau}\frac{Q}{k}\int_0^r\left(\frac{1}{r^2}\int_0^r r^2dr\right)dr+C_2 \tag{23}$$

where the constant C_2 is obtained within the Laplace domain as

$$C_2=\Psi(t)\left(q_0+\frac{\kappa}{\tau}\frac{Q}{6k}\xi^2\right)+\zeta\frac{\kappa}{\tau}\frac{Q}{3k}\xi \tag{24}$$

where

$$\Psi(t)=\begin{cases}\dfrac{t^{-\alpha}}{\Gamma(1-\alpha)}, & 0<\alpha<1,\\ \delta(t), & \alpha=1\end{cases}$$

Similarly, the function $\theta_t(r,t)$ satisfies the non-homogeneous differential equation

$$\frac{\partial^2\theta_t}{\partial t^2}+\frac{1}{\tau}\frac{\partial^\alpha\theta_t}{\partial t^\alpha}=\frac{\kappa}{\tau}\left[\frac{1}{r^2}\frac{\partial}{\partial r}\left(r^2\frac{\partial\theta_t}{\partial r}\right)\right] \tag{25}$$

subjected to homogenous boundary conditions given as

$$\theta_t(r,t=0)=0,\ \frac{\partial\theta_t}{\partial t}(r,t=0)=0 \tag{26}$$

$$\theta_t(r=\xi,t)+\zeta D_{RL}^{1-\alpha}\frac{\partial\theta_t}{\partial r}(r=\xi,t)=0 \tag{27}$$

Applying Laplace transform with respect to variable t leads to

$$\left(s^2+\frac{1}{\tau}s^\alpha\right)\bar{\theta}_t=\frac{\kappa}{\tau}\left[\frac{1}{r^2}\frac{\partial}{\partial r}\left(r^2\frac{\partial\bar{\theta}_t}{\partial r}\right)\right] \tag{28}$$

$$\bar{\theta}_t(r=\xi,t)+\zeta s^{1-\alpha}\frac{\partial\bar{\theta}_t}{\partial r}(r=\xi,t)=0 \tag{29}$$

Multiplying $J_0(r\,k_i)\,r^2$ to Eq. (28) and integrating with regards to r from 0 to a. Now on account of the operational property (refer to Appendix A) and inserting the boundary condition (29), one obtains

$$\bar{\bar{\theta}}_t(k_i,s)=\frac{1}{s^2+(1/\tau)s^\alpha+k_i^2} \tag{30}$$

Taking the Laplace inversion integral [39] of Eq. (30), one obtains

$$\bar{\theta}_t(k_i,t)=\frac{1}{2\pi i}\int_{c-i\infty}^{c+i\infty}\frac{\exp(st)}{s^2+(1/\tau)s^\alpha+k_i^2}ds \tag{31}$$

where c is greater than the real part of all the singularities of the integrand.

The integration path for $t\geq 0$ inside the principal branch of $s^\alpha(-\pi<\arg s<\pi)$ is depicted in Figure 2.

Let $\delta\to 0$ and $R\to\infty$. Since $\cos(.)\leq 0$ if $\pi/2\leq|.|<\pi$ and $\exp(st)/g(s)=o(1/R^2)$ if $R\to\infty$ the integral vanishes on the circular arcs with $o(1/R)$. Then $g(s)=s^2+(1/\tau)s^\alpha+k_i^2$ has exactly two zeros $s_{A/B}=-\mu\pm i\vartheta$ on the principal branch, which are simple, conjugate complex and placed in the open left half-plane.

http://doi.org/10.29369/ijrbat.2023.02.1.0015

To solve the Eq. (30), using the residue theorem lead to

$$\bar{\theta}_t(t) = \mathrm{Re}\, S_A\left(\frac{\exp(st)}{g(s)}\right) + \mathrm{Re}\, S_B\left(\frac{\exp(st)}{g(s)}\right) - \frac{1}{2\pi i}\lim_{\substack{R\to\infty \\ \delta\to 0}}\left[\int_{l_1}\frac{\exp(st)}{g(s)}dt + \int_{l_2}\frac{\exp(st)}{g(s)}dt\right] \quad (32)$$

Firstly consider $\bar{\theta}_1(t)$ as the sum of the first two terms of Eq. (32) and taking $\hat{a} = \mathrm{Re}[g'(s_A)]$ and $\hat{b} = \mathrm{Im}[g'(s_A)]$, one gets

$$\bar{\theta}_1(t) = \frac{2\exp(-\mu t)}{\hat{a}^2 + \hat{b}^2}[\hat{a}\cos(\vartheta t) + \hat{b}\sin(\vartheta t)] \quad (33)$$

Now consider $\bar{\theta}_2(t)$ as the last terms of Eq. (32), along $l_{A/B} : s = p\exp(\pm i\pi) \pm i\delta,\ p \in [0,\infty]$. If $\delta \to 0$ then $s^2 \to p^2,\ s^\alpha \to p^\alpha \exp(\pm i\pi\alpha) = p^\alpha[\cos(\pi\alpha) \pm i\sin(\pi\alpha)],\ ds \to dp$ and, one obtains

$$\bar{\theta}_2(t) = -\frac{1}{\pi}\mathrm{Im}\left[\int_0^\infty \frac{\exp(-pt)\,dp}{p^2 + (1/\tau)\,p^\alpha[\cos(\pi\alpha) \pm i\sin(\pi\alpha)] + k_i^2}\right] \quad (34)$$

Removing the imaginary number in the denominator by its conjugate, one gets

$$\bar{\theta}_2(t) = \frac{\sin(\pi\alpha)}{\pi\tau}\left[\int_0^\infty \frac{p^\alpha \exp(-pt)\,dp}{[p^2 + (1/\tau)\,p^\alpha(\cos(\pi\alpha) + k_i^2]^2 + [(1/\tau)p^\alpha\sin(\pi\alpha)]^2}\right] \quad (35)$$

Taking the sum of residues as $\bar{\theta}_s(t) = \bar{\theta}_1(t) + \bar{\theta}_2(t)$, one obtains

$$\bar{\theta}_t(k_i,t) = \frac{2\exp(-\mu t)}{\hat{a}^2 + \hat{b}^2}[\hat{a}\cos(\vartheta t) + \hat{b}\sin(\vartheta t)] + \frac{\sin(\pi\alpha)}{\pi\tau}\left[\int_0^\infty \frac{p^\alpha \exp(-pt)\,dp}{[p^2 + (1/\tau)\,p^\alpha(\cos(\pi\alpha) + k_i^2]^2 + [(1/\tau)p^\alpha\sin(\pi\alpha)]^2}\right] \quad (37)$$

Applying the inversion theorem (refer to Appendix A), one obtains

$$\theta_t(r,t) = \left(\frac{4}{\pi\xi^2}\right)\sum_{i=1}^\infty \frac{k_i^2}{h^2 + k_i^2}\frac{J_0(r\,k_i)}{[J'_{1/2}(\alpha_i)]^2}\bar{\theta}(k_i,t) \quad (38)$$

Taking the temperature as $\theta(r,t) = \theta_s(r) + \theta_t(r,t)$, one obtains

$$\theta(r,t) = -\frac{\kappa}{\tau}\frac{Q}{k}\int_0^r\left(\frac{1}{r^2}\int_0^r r^2 dr\right)dr + \left(\frac{4}{\pi\xi^2}\right)\sum_{i=1}^\infty \frac{k_i^2}{h^2 + k_i^2}\frac{J_0(r\,k_i)}{[J'_{1/2}(\alpha_i)]^2}\bar{\theta}(k_i,t) + \Psi(t)\left(q_0 + \frac{\kappa}{\tau}\frac{Q}{6k}\xi^2\right) + \zeta\frac{\kappa}{\tau}\frac{Q}{3k}\xi \quad (39)$$

and unknown temperature function on the outer curved surface is given by

$$\theta(a,t) = -\frac{\kappa}{\tau}\frac{Q}{k}\left[\int_0^a\left(\frac{1}{r^2}\int_0^r r^2 dr\right)dr\right] + \left(\frac{4}{\pi\xi^2}\right)\sum_{i=1}^\infty \frac{k_i^2}{h^2 + k_i^2}\frac{J_0(a\,k_i)}{[J'_{1/2}(\alpha_i)]^2}\bar{\theta}(k_i,t) + \psi(t)\left(q_0 + \frac{\kappa}{\tau}\frac{Q}{6k}\xi^2\right) + \zeta\frac{\kappa}{\tau}\frac{Q}{3k}\xi \quad (40)$$

Substituting Eq. (40) into $\theta(r=a,t) = \Theta(t)$, one can get the unknown temperature $T(r=a,t) = \int_0^t f(t-\gamma)\Theta(\gamma)\,d\gamma$ at the ball surface.

Displacement and stress field solution

Let $u_r = u_r(r,t)$ be a component of displacement, and expressed [40] as

$$u_r(r,t) = \alpha_t K\frac{1}{r^2}\int_0^r T(r,t)r^2 dr + 2\alpha_t\left(\frac{1-2\upsilon}{1-\upsilon}\right)\frac{r}{a^3}\int_0^a T(r,t)r^2 dr \quad (41)$$

that satisfies the displacement equation

$$\frac{d}{dr}\left[\frac{1}{r^2}\frac{d}{dr}(r^2 u_r)\right] = K\frac{dT}{dr} \quad (42)$$

in which $K = [(1+\upsilon)/(1-\upsilon)]\alpha_t$ is the restraint coefficient, α_t and υ denote the coefficient of linear thermal expansion and Poisson's ratio, respectively.

Let $\sigma_{rr}, \sigma_{\theta\theta}, \sigma_{\varphi\varphi}$ be the components of stress, and expressed [40] as

$$\sigma_{rr}(r,t) = \frac{\alpha_t E}{1-v}\left[\frac{2}{a^3}\int_0^a T(r,t)r^2 dr - \frac{1}{r^3}\int_0^r T(r,t)r^2 dr\right]$$

$$\sigma_{\theta\theta}(r,t) = \sigma_{\varphi\varphi}(r,t) = \frac{\alpha_t E}{1-v}\left[\frac{2}{a^3}\int_0^a T(r,t)r^2 dr - \frac{1}{r^3}\int_0^r T(r,t)r^2 dr - T(r,t)\right] \quad (43)$$

in which traction-free boundary conditions are $\sigma_{rr}(r=a,t) = 0$.

Substituting $T(r=a,t)$ into Eqs. (41) and (43), one can obtain the ball surface's unknown displacement and thermal stresses.

http://doi.org/10.29369/ijrbat.2023.02.1.0015

Numerical results, discussion and remarks

For the sake of simplicity of numerical computations, we introduce the following nondimensional parameters as

$$\bar{r} = r/a, \bar{t} = t\kappa/a^2, \bar{T} = T/T_0, \bar{u}_i = u_i/KT_0a\,(i = r),$$
$$\bar{\sigma}_{ii} = \sigma_{ii}/E\alpha_t T_0\,(i = r, \theta, \varphi) \quad (44)$$

with physical parameters for the solid ball as $a =$ 2m and the surrounding temperature as $T_0 = 150^{o}$C.Substituting the value of Eq. (44) in Eqs. (39), (41) and (43), one obtains the expressions for the temperature, displacement and thermal stresses for our numerical discussion. The numerical computations have been carried out for Aluminium (pure) ball with the thermo-mechanical properties: modulus of elasticity E = 70 GPa, Poisson's ratio υ = 0.35, thermal expansion coefficient α = $23\times10^{-6}/^{0}$C, thermal diffusivity κ = 84.18×10^{-6} m^2s^{-1} and thermal conductivity λ = $204.2Wm^{-1}K^{-1}$. The $k_i = \alpha_i/a =$ 2.61736, 5.51894, 8.65373, 11.7915, 14.9309, 18.0711, 21.2116, 24.3525, 27.4935, 30.6346, 33.7758, 36.9171, 40.0584, 43.1998, 46.3412, 49.4826are the positive and real roots of the transcendental equation $k_i J_n'(ak_i) + hJ_n(ak_i) = (\alpha_i/a)J_n'(\alpha_i) + hJ_n(\alpha_i) = 0$. Numerical calculations were performed for all variables to examine the effect of heating on the plate, and numerical results are illustrated in the accompanying figures employing MATHEMATICA software. Figures 3-14 illustrates the numerical results in the graphical form for temperature distribution, displacement profile and variation in stress distribution in a spherical ball under the physical Robin boundary condition. Figures 3-4 denote the temperature distribution against the fractional-order α for the various values of $\bar{r}$ and τ, both with and without an internal heat source. It can be noticed in both the figures that under the absence of a heat source, the temperature is zero at the initial stages, starts gradually increasing, attains maxima at a different value of $\bar{r}$ and τ , and it finally decreases asymptotically. On the other hand, under a heat source, the temperature has a specific value at the initial stages and behaves the same as it did without a heat source. The gradual increase in the temperature for both with or without heat source for a certain value α may be due to the body's geometry's ability to hold the heat.

Figures 5-6 represent the value of temperature along dimensionless radial direction for different values of α and τ, for both with and without a heat source. The hike in the sinusoid pattern may be due to the internal heat generation accumulation but gets flatten at the ball's outer core. Figures 7-8 depict the variation in the temperature distribution along time $\bar{t}$ for different values of α and τ, with and without an internal heat source. From the figure, it is clearly understood that the temperature value increases linearly with the increase in the time in the absence of internal heat source and surrounding temperature, which defines the close correlation between the time and temperature. In contrast, the presence of heat generation as well as surround heat generates a gradual increase curve for the value of temperature and attaining a uniformity after some time.

Figure 9 gives a variation of dimensionless displacement $\bar{u}_r$ along the radial direction for different values α with and without a heat source. The effect of the temperature distribution in the presence of internal heat generation causes a dramatic change in displacement compared to the change observed in the absence of a heat source. It can be easily seen that no displacement is observed initially, but along the radial direction, it increases and then becomes stagnant at a particular value of $\bar{r}$ due to the effect of temperature distribution

http://doi.org/10.29369/ijrbat.2023.02.1.0015

on the ball. Figure 10 shows the variation in the displacement distribution $\bar{u}_r$ along the τ direction for different values of $\bar{r}$ both availability or absence of an internal heat source. One can observe the change taking place in the displacement with an increase in the relaxation time. Initially, the displacement is none and slowly increases asymptotically due to the effect of the temperature distribution.

Figure 11 depicts the relation between the radial stresses along the radial direction for the different values of α when $t = \tau = 1$ in both when internal heat sources are present or absent. In both cases, the difference in the stresses can be readily noticeable. The nature of the stresses is such that it starts accumulating stability at the ball's outer end with a gradual increase that can be seen from low initiation. Figure 12 gives variation in radial stresses along relaxation time for various values of α for both, with and without a heat source. The gradual decreasing nature in the plot can be observed at zero relaxation time no, or a negligible amount of stresses are found, which decreases as the relaxation time increases, ultimately defining the importance of relation time. Figures 13-14 show the relation between $\bar{\sigma}_{\theta\theta} = \bar{\sigma}_{\varphi\varphi}$ along $\bar{r}$ and τ for different values of α. The graph's nature is the same in both the figures for both, with and without a heat source. The stresses' values are very low initially and increase slowly at the outer end due to the accumulation of the surrounding temperature.

Deduction and validation of the results :

This section corresponds to the deduction of results obtained above to that regarding the classical uncoupled thermoelasticity model and classical Cattaneo-Vernotte thermoelasticity theory for a homogeneous sphere.

(i) Taking $\tau = 0$ and $\alpha = 1$ in Eq. (7), the equation reduces to the classical Fourier heat conduction model [30].

(ii) Taking $\alpha = 1$ in Eq. (7), the equation results in the classical Cattaneo-Vernotte heat conduction model [19,20].

The present deduced thermoelastic solutions agree with the key derived by Ghonge and Ghadle [41] for an isotropic, homogeneous, elastic sphere. This work combines a fractional-order constitutive model with the standard continuity equation. However, recent investigations [47,48] show the coexistence of the non-Fourier constitutive model and non-trivial continuity equation based on the Boltzmann transport theory. The results illustrate that the constitutive model and continuity equation are not independent of each other, which is not considered by this work.

CONCLUSION :

In this problem, the fractional Cattaneo model is derived for studying the thermoelastic response of a rigid ball that is internally impacted by an assigned temperature. At the same time, heat supply appears as a source in the energy equation. The theory of integral transformation is used to obtain the analytical solution for the fractional Cattaneo and classical Fourier models. The temperature distribution dependence and its thermoelastic response on the fractional-order parameter and relaxation time are studied for different times and positions. It is observed that the fractional Cattaneo model gives the continuous temperature and thermal stress variation irrespective of the fractional-order parameter. It is also detected that the heat flux flows from higher temperatures to lower for the fractional Cattaneo and classical Fourier models.

REFERENCES:

G. Stolz, Numerical solutions to an inverse problem of heat conduction for simple shapes, *J. Heat Transfer*, Vol. 82, No. 1, pp. 20-25, 1960.DOI: 10.1115/1.3679871.

http://doi.org/10.29369/ijrbat.2023.02.1.0015

D. Necsulescu, *Advanced Mechatronics: Monitoring and Control of Spatially Distributed Systems*, Singapore: World Scientific Company, 2009.

K. Woodbury, *Inverse Engineering Handbook*, Boca Raton: CRC Press, 2003.

M. Ozisik and H. Orlande, *Inverse Heat Transfer: Fundamentals and Applications*, New York ; Taylor & Francis, 2000.

J. Beck, B. Blackwell and JR Charles, *Inverse Heat Conduction: Ill-posed Problems*. New York; John Willey & Sons, 1985.

L. Torsten, A. Mhamdi, and W. Marquardt, Design, formulation, and solution of multidimensional inverse heat conduction problems, *Numer. Heat Tr-B Fund.*, Vol. 47, pp. 111 - 133, 2005.DOI: 10.1080/10407790590883351.

X. Lu, and P. Tervola, Transient heat conduction in the composite slab-analytical method, *J Phys Math Gen*, Vol. 38, pp. 81 - 96, 2005.DOI: 10.1088/0305-4470/38/1/005.

K. W. Khobragade, V. Varghese and N. W. Khobragade, An inverse transient thermoelastic problem of a thin annular disc, Appl. Math. E-Notes, Vol. 6, pp. 17-25, 2006.

P. L. Woodfield, M. Monde, and Y. Mitsutake, Improved analytical solution for inverse heat conduction problems on thermally thick and semi-infinite solids, *Int. J. Heat Mass Transfer*, Vol. 49, pp. 2864 - 2876, 2006.DOI: 10.1016/j.ijheatmasstransfer.2006.01.050.

R. Pourgholi, and M. Rostamian, A numerical technique for solving IHCPs using Tikhonov Regularization Method, *Appl. Math. Model*, Vol. 34, pp. 2102 - 2110, 2010. DOI: 10.1016/j.apm.2009.10.022.

S. Danaila, and A. Chira, Mathematical and numerical modeling of inverse heat conduction problem, *INCAS BULLETIN*, Vol. 6, pp. 23–39, 2014.DOI: 10.13111/2066-8201.2014.6.4.3.

M. Ivanchov and N. Kinash, Inverse problem for the heat-conduction equation in a rectangular domain, *Ukr. Math. J.*, Vol. 69, No. 12, 2018.DOI: 10.1007/s11253-018-1476-1.

H. Chen, I. Jay, J. Frankel, and M. Keyhani, Nonlinear inverse heat conduction problem of surface temperature estimation by calibration integral equation method, *Numer. Heat Tr-B Fund.*, Vol. 73, No. 5, pp. 263–291, 2018.DOI: 10.1080/10407790.2018.1464316.

C. Chang, C. Liu, and C. Wang, Review of computational schemes in inverse heat conduction problems, *Smart Sci.*, Vol. 6, No. 1, pp. 94–103, 2018.DOI: 10.1080/23080477.2017.1408987.

S. Kukla and U. Siedlecka, Laplace transform solution of the problem of time-fractional heat conduction in a two-Layer slab, *J. Appl. Comput. Mech.*, Vol. 14, No. 4, pp. 105-113, 2015.DOI: 10.17512/jamcm.2015.4.10.

E. Hoashi, T. Yokomine, A. Shimizu, and T. Kunugi, Numerical analysis of wave-type heat transfer propagating in a thin foil irradiated by short-pulsed laser, *Int. J. Heat Mass Transf.*, Vol. 46, No. 21, pp. 4083–4095, 2003. DOI: 10.1016/S0017-9310(03)00225-4.

X. Ai and B. Q. Li, Numerical simulation of thermal wave propagation during laser processing of thin films, *J. Electron. Mater.*, Vol. 34, No. 5, pp. 583–591, 2005. DOI: 10.1007/s11664-005-0069-6.

T. T. Lam and E. Fong, Application of solution structure theorem to non-Fourier heat conduction problems: Analytical

approach, *Int. J. Heat Mass Transf.*, Vol. 54, No. 23–24, pp. 4796–4806, 2011. DOI: 10.1016/j.ijheatmasstransfer.2011.06.028.

T. T. Lam, A unified solution of several heat conduction models, *Int. J. Heat Mass Transf.*, Vol. 56, No. 1–2, pp. 653–666, 2013. DOI: 10.1016/j.ijheatmasstransfer.2012.08.055.

C. Cattaneo, Sur uneForme de I'equation de la Chaleur Eliminant le Paradoxed'une Propagation Instantanee', *ComptesRendus de l'Académie des Sciences*, Vol. 247, pp. 431-433, 1958.

P. Vernotte, Les paradoxes de la théorie continue de l'équation de la chaleur, *C. R. Acad. Sci. Paris*, Vol. 246, pp. 3154-3155, 1958.

A. Compte and R. Metzier, The generalized Cattaneo equation for the description of anomalous transport processes, *J. Phys. A: Math. Gen.*, Vol. 30, pp. 7277-7289, 1997.

Y. Z. Povstenko, Fractional Cattaneo-type equations and generalized thermoelasticity, *J. Therm. Stresses*, Vol. 34, No. 2, pp. 97-114, 2011. DOI: 10.1080/01495739.2010.511931

T. N. Mishra and K. N. Rai, Numerical solution of FSPL heat conduction equation for analysis of thermal propagation, *Appl. Math. Comput.*, Vol. 273, pp. 1006–1017, 2016. DOI: 10.1016/j.amc.2015.10.082.

H.-T. Qi, H.-Y. Xu, and X.-W. Guo, The Cattaneo-type time fractional heat conduction equation for laser heating, *Comput. Math. Appl.*, Vol. 66, No. 5, pp. 824–831, 2013. DOI: 10.1016/j.camwa.2012.11.021.

H. T. Qi, H. Y. Xu and X. W. Guo, The Cattaneo-type time fractional heat conduction equation for laser heating, *Comput. Math. Appl.*, Vol. 66, pp. 824–831, 2013.DOI: 10.1016/j.camwa.2012.11.021

H. T. Qi, and X.W. Guo, Transient fractional heat conduction with generalized Cattaneo model, *Int. J. Heat Mass Transfer*, Vol. 76, pp. 535–539, 2014. DOI: 10.1016/j.ijheatmasstransfer.2013.12.086.

H. Y. Xu, H. T. Qi, and X. Y. Jiang, Fractional Cattaneo heat equation in a semi-infinite medium, *Chin. Phys. B*, Vol. 22, pp. 014401, 2013. DOI: 10.1088/1674-1056/22/1/014401

G. Y. Xu, J. B. Wang, and Z. Han, Study on the transient temperature field based on the fractional heat conduction equation for laser heating, *Appl. Math. Mech.*, Vol. 36, pp. 844–849, 2015.

H. R. Ghazizadeh, M. Maerefat, and A. Azimi, Explicit and implicit finite difference schemes for fractional Cattaneo equation, *J. Comput. Phys.*, Vol. 229, No. 19, pp. 7042–7057, 2010. DOI: 10.1016/j.jcp.2010.05.039.

M. N. Özisik, *Heat Conduction*, John Wiley & Sons, New York, 1993.

D. Y. Tzou, Thermal shock phenomena under high rate response in solids, *Ann. Rev. Heat Transf.*, Vol. 4, pp. 111–185, 1992.DOI: 10.1615/AnnualRevHeatTransfer.v4.50

M. E. Gurtin and A. C. Pipkin, A general theory of heat conduction with finite wave speeds, *Arch. Rational Mech. Anal.*, Vol. 31, pp. 113–126, 1968. DOI: 10.1007/BF00281373

A. Compte, A. Metzler, and J. Camacho, Biased continuous time random walks between

parallel plates, Phys. Rev. E, Vol. 56, No. 2, pp. 1445-1454, 1997.

M. N. Özisik, D. Y. Tzou, On the wave theory in heat conduction, *J. Heat Transf.*, Vol. 116, pp. 526–535, 1994.DOI: 10.1115/1.2910903

S. Kaliski, Wave equations of thermoelasticity, *Bull. Acad. Polon. Sci. Ser. Sci. Techn.*, Vol. 13, pp. 253-260, 1965.

H. W. Lord and Y. Shulman, A generalized dynamical theory of thermoelasticity, *J. Mech. Phys. Solids*, Vol. 15, pp. 299-309, 1967.

I. Podlubny, *Fractional Differential Eq*uations, Academic Press, New York, 1999.

Y. Povstenko, Axisymmetric solutions to fractional diffusion-wave equation in a cylinder under Robin boundary condition, *Eur. Phys. J. Spec. Top.*, Vol. 222, No. 8, pp. 1767–1777, 2013. DOI: 10.1140/epjst/e2013-01962-4.

Y. Z. Povstenko, Axisymmetric Solutions to Time-Fractional Heat Conduction Equation in a Half-Space under Robin Boundary Conditions, *Int. J. Differ. Equ.*, Vol. 2012, pp. 1–13, 2012. DOI: 10.1155/2012/154085.

Y. Povstenko, Fundamental solutions to the fractional heat conduction equation in a ball under Robin boundary condition, *Open Math.*, Vol. 12, No. 4, 2014. DOI: 10.2478/s11533-013-0368-8.

H. Beyer and S. Kempfle, Definition of physically consistent damping laws with fractional derivatives, *ZAMM - J. Appl. Math. Mech.*, Vol. 75, No. 8, pp. 623–635, 1995. DOI: 10.1002/zamm.19950750820.

N. Noda, R. B. Hetnarski, Y. Tanigawa, *Thermal stresses*, 2nd edition, Taylor and Francis, New York, 2003.

B.E. Ghonge and K.P. Ghadle, An inverse transient thermoelastic problem of solid sphere, *Bulletin of Pure and Applied Sciences*, vol.29, no.1, pp. 1-9, 2010.

I. N. Snedden, *The Use of Integral Transforms*, McGraw-Hill Book Co., New York, Ch. 5, 1972.

I. H. Chen, Modified Fourier-Bessel series and finite spherical Hankel transform, *Int. J. Math. Educ. Sci. Technol.*, Vol. 13, No. 3, pp. 281-283, 1982. DOI: 10.1080/0020739820130307

S. N. Li, B.Y. Cao, Fractional Boltzmann transport equation for anomalous heat transport and divergent thermal conductivity, *Int. J. Heat Mass Transf.*, Vol. 137, pp. 84-89, 2019.

S. N. Li, B.Y. Cao, Fractional-order heat conduction models from generalized Boltzmann transport equation, *Philos. Trans. R. Soc. A*, Vol 378, 20190280, 2020.

Appendix A

The transformation and its essential property

Here, the Fourier-Bessel series and Hankel transform [42] to spherical coordinates [43] are extended, which is more suitable to third kind boundary conditions. Assuming a finite interval $0 < r < a$ in the spherical coordinate lead to the spherical-Bessel series representation of a function $f(r)$, which can be stated as

$$f(r) = \sum_{i=1}^{\infty} c_i J_n(r k_i) \qquad \text{(A.1)}$$

where c_i are the coefficients to be determined and $J_n(r k_i)$ is a spherical Bessel function of order n. The eigenvalues $k_i = \alpha_i / a$ are defined by the solutions of

$$k_i J_n'(a k_i) + h J_n(a k_i) = (\alpha_i / a) J_n'(\alpha_i) + h J_n(\alpha_i) = 0 \qquad \text{(A.2)}$$

in which α_i is an i^{th} root of the spherical Bessel function and prime denotes the differentiation of the Bessel function.

http://doi.org/10.29369/ijrbat.2023.02.1.0015

Multiplying Eq. (A.1) by $J_n(r\,k_j)$, integrating both sides of the result from 0 to a, and using the orthogonal property of Bessel functions, then taking $n=0$ one obtains

$$\int_0^a f(r)J_0(r\,k_i)\,r^2dr=\frac{c_i\,\pi}{2k_i}\int_0^a[J_{1/2}(r\,k_i)]^2\,r\,dr \qquad \text{(A.3)}$$

Following the procedure of Chen [43], one obtains the series coefficients as

$$c_i=\frac{4}{\pi a^2}\frac{k_i}{[J'_{1/2}(\alpha_i)]^2}\int_0^a f(r)J_0(r\,k_i)\,r^2dr \qquad \text{(A.4)}$$

Substituting the value of c_i into Eq. (1) gives

$$f(r)=\left(\frac{4}{\pi a^2}\right)\sum_{i=1}^{\infty}\frac{k_i}{[J'_{1/2}(\alpha_i)]^2}\int_0^a f(r)J_0(r\,k_i)\,r^2dr \qquad \text{(A.5)}$$

Thus, the zero-order finite Hankel transform and its inverse are defined as

$$\bar{f}(k_i)=\int_0^a f(r)J_0(r\,k_i)\,r^2dr \qquad \text{(A.6)}$$

$$f(r)=\left(\frac{4}{\pi a^2}\right)\sum_{i=1}^{\infty}\frac{k_i^2\,\bar{f}(k_i)}{h^2+k_i^2}\frac{J_0(r\,k_i)}{[J'_{1/2}(\alpha_i)]^2} \qquad \text{(A.7)}$$

and the only property which will be made use

$$\mathrm{A}_0\left\{\frac{\partial^2 f}{\partial r^2}+\frac{2}{r}\frac{\partial f}{\partial r}\right\}=-k_i^2\,\bar{f}+aJ_0(a\,k_i)\left[\frac{\partial f}{\partial r}+hf\right]_{r=a} \qquad \text{(A.8)}$$

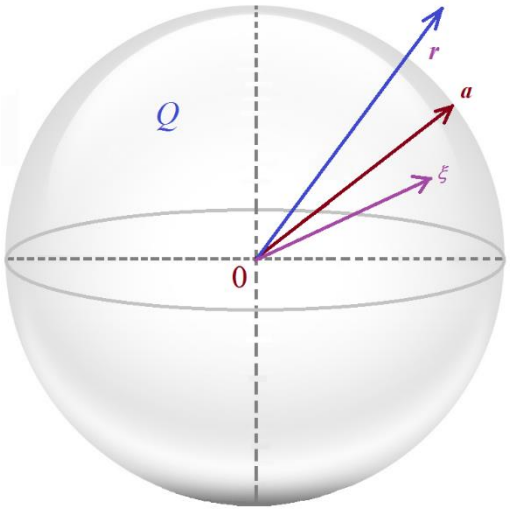

Figure 1 profile of a spherical metal ball

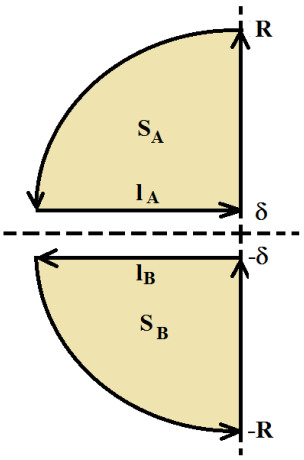

Figure 2 Integration path

http://doi.org/10.29369/ijrbat.2023.02.1.0015

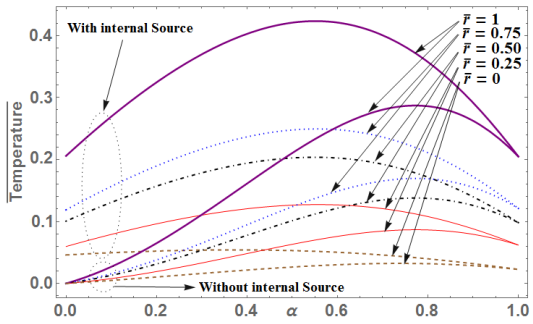

Fig. 3 Temperature distribution along α for different values of $\bar{r}$ ($\tau = 1$, $t = 0.6$).

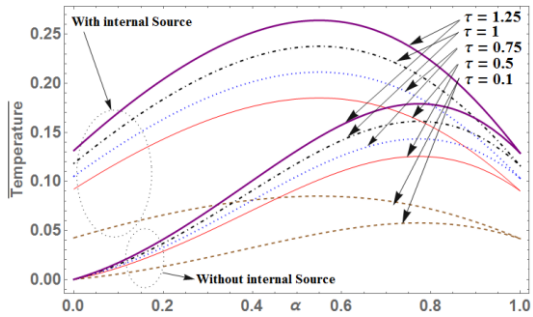

Fig. 4 Temperature profile along α for different values of τ ($\bar{r} = 0.8$, $t = 0.6$).

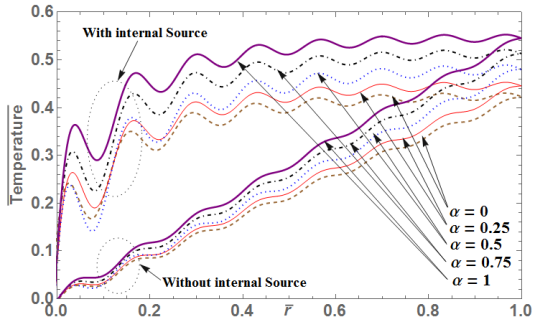

Fig. 5 Temperature along $\bar{r}$ for different values of α ($\tau = 0.75$, $t = 1$).

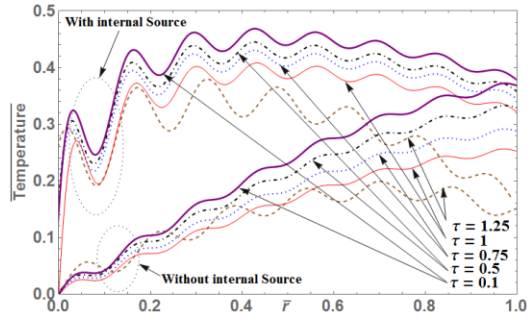

http://doi.org/10.29369/ijrbat.2023.02.1.0015

Fig. 6 Temperature variation along $\bar{r}$ for various values of τ ($\alpha = 0.8$, $t = 1$).

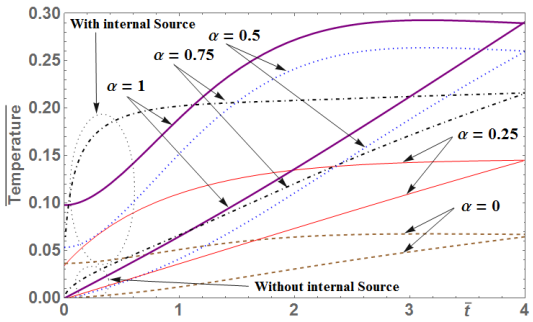

Fig. 7 Temperature distribution along $\bar{t}$ for different values of α ($\tau = 1$, $t = 0.6$).

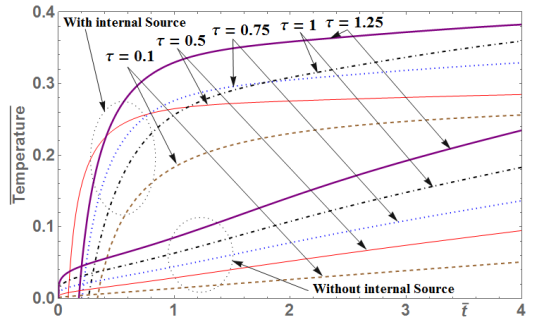

Fig. 8 Temperature profile along $\bar{t}$ for different values of τ ($\alpha = 0.8$, $\bar{r} = 1$).

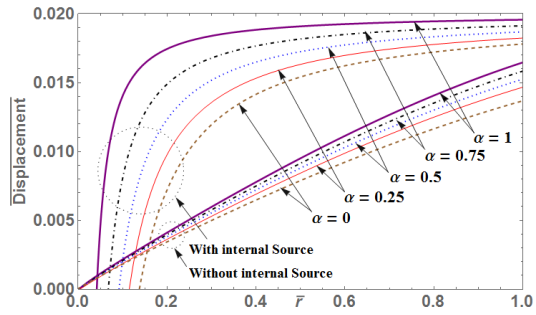

Fig. 9 Variation of displacement $\bar{u}_r$ along the $\bar{r}$ direction for different α .

http://doi.org/10.29369/ijrbat.2023.02.1.0015

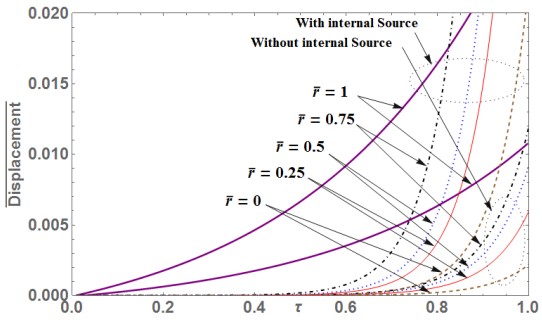

Fig. 10 Displacement distribution $\bar{u}_r$ along the τ direction for different $\bar{r}$.

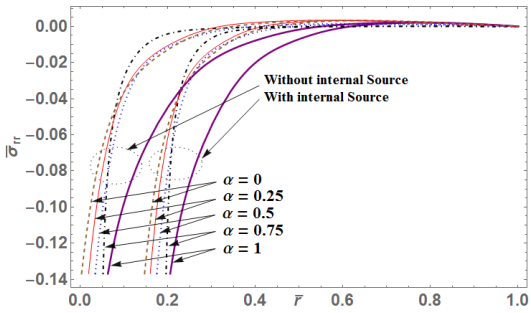

Fig. 11 $\bar{\sigma}_{rr}$ along $\bar{r}$ for different values of α ($\tau = 1$, $t = 1$).

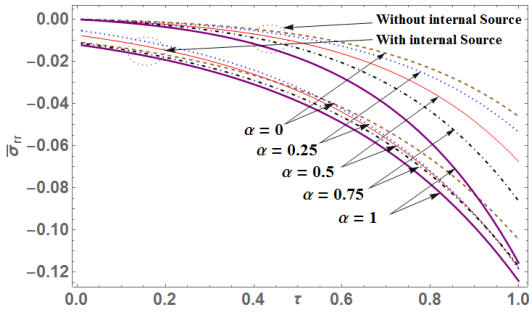

Fig. 12 $\bar{\sigma}_{rr}$ profile along τ for various values of α ($\bar{r} = 0.4$, $t = 0.6$).

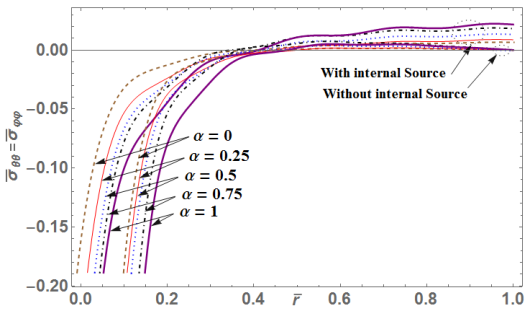

Fig. 13 $\bar{\sigma}_{\theta\theta} = \bar{\sigma}_{\varphi\varphi}$ along $\bar{r}$ for different values of α ($\tau = 0.75$, $t = 1$).

http://doi.org/10.29369/ijrbat.2023.02.1.0015

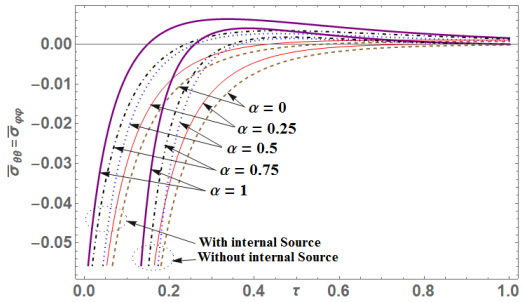

Fig. 14 $\bar{\sigma}_{\theta\theta}=\bar{\sigma}_{\varphi\varphi}$ ***along*** τ ***for various values of*** α ***(***$\bar{r}=0.6$ **,** $t=0.8$ ***)***

http://doi.org/10.29369/ijrbat.2023.02.1.0015